BMC Complementary Medicine and Therapies

RESEARCH

Open Access

In vitro cytotoxic effect of stigmasterol derivatives against breast cancer cells

Nondumiso Premilla Dube[1], Vuyelwa Jacqueline Tembu[1], Getrude R Nyemba[2], Candace Davison[2], Goitsemodimo Herckious Rakodi[1], Douglas Kemboi[1,3], Jo-Anne de la Mare[2], Xavier Siwe-Noundou[4] and Amanda-Lee Ezra Manicum[1*]

Abstract

Background Stigmasterol is an unsaturated phytosterol that belong to the class of tetracyclic steroids abundant in *Rhoicissus tridentata*. Stigmasterol is an important constituent since it has shown impressive pharmacological effects such as anti-osteoarthritis, anticancer, anti-diabetic, anti-inflammatory, antiparasitic, immunomodulatory, antifungal, antioxidant, antibacterial, and neuroprotective activities. Furthermore, due to the presence of π system and hydroxyl group, stigmasterol is readily derivatized through substitution and addition reactions, allowing for the synthesis of a wide variety of stigmasterol derivatives.

Methods Stigmasterol (**1**) isolated from *Rhoicissus tridentata* was used as starting material to yield eight bio-active derivatives (**2**–**9**) through acetylation, epoxidation, epoxide ring opening, oxidation, and dihydroxylation reactions. The structures of all the compounds were established using spectroscopic techniques, NMR, IR, MS, and melting points. The synthesized stigmasterol derivatives were screened for cytotoxicity against the hormone receptor-positive breast cancer (MCF-7), triple-negative breast cancer (HCC70), and non-tumorigenic mammary epithelial (MCF-12 A) cell lines using the resazurin assay.

Results Eight stigmasterol derivatives were successfully synthesized namely; Stigmasterol acetate (**2**), Stigmasta-5,22-dien-3,7-dione (**3**), 5,6-Epoxystigmast-22-en-3β-ol (**4**), 5,6-Epoxystigmasta-3β,22,23-triol (**5**), Stigmastane-3β,5,6,22,23-pentol (**6**), Stigmasta-5-en-3,7-dion-22,23-diol (**7**), Stigmasta-3,7-dion-5,6,22,23-ol (**8**) and Stigmast-5-ene-3β,22,23-triol (**9**). This is the first report of Stigmasta-5-en-3,7-dion-22,23-diol (**7**) and Stigmasta-3,7-dion-5,6,22,23-ol (**8**). The synthesized stigmasterol analogues showed improved cytotoxic activity overall compared to the stigmasterol (**1**), which was not toxic to the three cell lines tested (EC_{50} > 250 µM). In particular, 5,6-Epoxystigmast-22-en-3β-ol (**4**) and stigmast-5-ene-3β,22,23-triol (**9**) displayed improved cytotoxicity and selectivity against MCF-7 breast cancer cells (EC_{50} values of 21.92 and 22.94 µM, respectively), while stigmastane-3β,5,6,22,23-pentol (**6**) showed improved cytotoxic activity against the HCC70 cell line (EC_{50}: 16.82 µM).

Conclusion Natural products from *Rhoicissus tridentata* and their derivatives exhibit a wide range of pharmacological activities, including anticancer activity. The results obtained from this study indicate that molecular modification of

*Correspondence:
Amanda-Lee Ezra Manicum
dubendumi@gmail.com; ManicumAE@tut.ac.za

Full list of author information is available at the end of the article

stigmasterol functional groups can generate structural analogues with improved anticancer activity. Stigmasterol derivatives have potential as candidates for novel anticancer drugs.

Keywords Stigmasterol, Cytotoxicity, MCF-7, HCC70, MCF-12A

Introduction

Rhoicissus tridentata is a deciduous shrub in the Vitaceae family, widely distributed throughout the Eastern region of southern Africa [1]. It is widely used in African medicinal systems to treat various ailments including erectile dysfunction, pains, swelling, cuts, wounds, kidney and bladder complications, stomach ailments, and livestock diseases, as well as for gynaecological purposes [2–7]. The medicinal uses of *R. tridentata* were attributed to the presence of bioactive compounds such as terpenoids, alkaloids and flavonoids, which showed promising anti-cancer, antioxidant, and anti-inflammatory activities [7–12]. The aqueous root extract of *R. tridentata* had the strongest antiproliferative effect, inhibiting HepG2 cell growth by 96.27%, while the methanol extract inhibited proliferation by 87.01% [2]. Modification of natural product structures leads to the discovery of novel agents with improved cytotoxicity in resistant tumours, decreased toxicity, and improved solubility [13, 14]. In this study, the roots of *R. tridentata* were phytochemically investigated and afforded stigmasterol in good yield. Stigmasterol was then selected as a candidate for synthetic modification with the aim of enhancing the anticancer activity.

Stigmasterol is an unsaturated phytosterol that belongs to the steroids class. It is a secondary metabolite that was isolated for the first time in 1906 in Calabarbohne by Adolf Wind Form and A. Hauth [15], and has since been isolated as the common compound from various medicinal plants [16]. Stigmasterol (stigmasta-5,22-dien-3β-ol, $C_{29}H_{48}O$), also known as Wulzen anti-stiffness factor or stigmasterin, is characterized by the presence of a hydroxyl group in position C-3 of the steroid skeleton. It also has double bonds in positions 5, 6 of the B ring, and in position 22, 23 in the alkyl substituent, as well as an isoprenyl tail (Fig. 1) [15, 16].

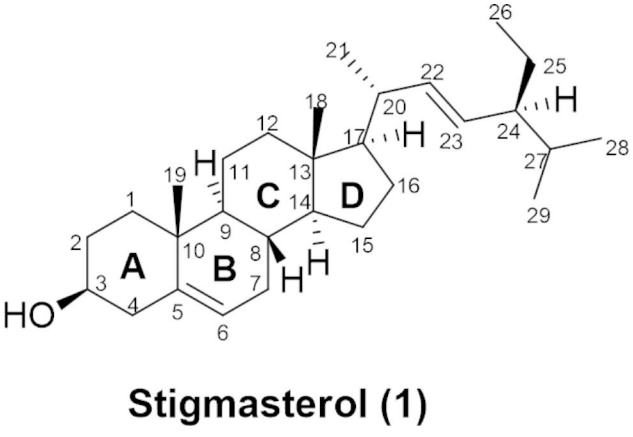

Stigmasterol (1)

Fig. 1 Chemical structure of Stigmasterol (**1**)

Stigmasterol is used in various chemical manufacturing processes which are designed to generate numerous synthetic and semi-synthetic compounds for the pharmaceutical industry [15, 17]. It serves as a precursor in the synthesis of hormones such as progesterone as well as an intermediate in the biosynthesis of androgens, corticoids, oestrogens [18] and in the synthesis of vitamin D_3 [15].

Stigmasterol has been investigated for its pharmacological prospects such as anti-osteoarthritic, immunomodulatory, cytotoxicity, antitumor, antiparasitic, antibacterial, antifungal, anti-diabetic, antimutagenic, antioxidant, anti-inflammatory and neuroprotective effects via in vitro and in vivo assays and molecular docking studies [15, 16, 19–23]. These studies unveiled the potential of stigmasterol as a key drug lead compound in the management of various illnesses, particularly in cancer therapy. In recent years, the anticancer potential of stigmasterol on numerous cancers was revealed through the different potential mechanisms of action [16]. This compound suppresses the development of various cancers, including gastric cancer [24], hepatoma [25], endometrial adenocarcinoma [26], breast cancer [26, 27], cholangiocarcinoma [28], skin cancer [29], gall bladder carcinoma [30], cervical cancer [27] and prostate cancer [31].

Stigmasterol isolated from the *Typhonium flagelliforme* mutant plant was found to be more effective against the human breast cancer MCF-7 cell line with an IC_{50} value of 0.1623 µM than cisplatin with an IC_{50} value of 13.2 µM [32, 33]. Stigmasterol can induce oxidative stress in MCF-7 cells, which leads to apoptosis. A competitive activator with a single high-affinity binding site on FXR and hydrophobic interactions facilitates this [32]. Li et al. [24] reported that stigmasterol suppressed proliferation and induced apoptosis in the human gastric cancer cell line SNU-1 through modulation of the JAK/STAT signalling pathway with an IC_{50} value of 15 µM. According to Bae et al. [34], stigmasterol can reduce the growth of human ovarian cancer cells ES2 and OV90 by 50% at a treatment concentration of 20 µg/mL, dose-dependently inducing apoptosis of ovarian cancer cells by causing mitochondrial malfunction, ROS production, and calcium overload in the mitochondria and cytosol.

In addition to stigmasterol, some of its derivatives, including stigmasta-5,22-dien-3,7-dione (**3**), 5,6-epoxystigmasta-3β,22,23-triol (**5**) and stigmast-5-ene-3β,22,23-triol (**9**) were also tested for their

pharmacological aspects and showed promising activity. Stigmasta-5,22-dien-3,7-dione (**3**) was screened for its immunomodulatory potential by Donkwe et al. [35]. Compound **3** displayed moderate inhibitory activity on the oxidative burst of the whole blood (IC_{50}=15.6±2.1 μM) compared to the control ibuprofen (IC_{50}=12.1 μM). In a study conducted by O'Callaghan et al. [36] to evaluate the cytotoxicity of oxidized derivatives of stigmasterol in the U937 human monocytic cell line using the Fluorescein Diacetate/Ethidium Bromide (FDA/EtBr) staining assay, 5,6-epoxystigmasta-3*β*,22,23-triol (**5**) and stigmast-5-ene-3*β*,22,23-triol (**9**), were found to induce a significant ($p<0.05$) level of cell death as compared to the untreated control. Stigmast-5-ene-3*β*,22,23-triol (**9**) caused a significant reduction ($p<0.05$) in cell viability at each of the three concentrations employed (30, 60, and 120 μM), reducing cell viability to 52.3% at the highest concentration. The 5,6-epoxystigmasta-3*β*,22,23-triol (**5**) significantly reduced cell viability ($p<0.05$) at the 60 and 120 μM concentrations. The mode of cell death following staining with Hoechst 33,342 was identified as apoptosis in cells incubated with 5,6-epoxystigmasta-3*β*,22,23-triol (**5**) [36].

Furthermore, because of the pharmacophores present, such as alkene bonds and the hydroxyl group, Stigmasterol is readily derivatized through substitution and addition reactions, allowing for the synthesis of a wide variety of stigmasterol derivatives. As a result, stigmasterol was selected as a candidate for synthetic modification. Eight derivatives of Stigmasterol (**1**) were successfully synthesized via acetylation, oxidation, epoxidation and ring-opening and dihydroxylation of the epoxide, to enhance their anticancer activity. The generated products were characterized using spectroscopic techniques and screened for anticancer activity against the MCF-7 and HCC70 breast cancer cell lines in comparison to the MCF-12 A non-cancerous breast epithelial cell line.

Methods and materials

General experimental procedures

Column chromatography was performed using silica gel (Kieselgel 40–63 μm, Macherey-Nagel, Germany). Thin Layer Chromatography (TLC) was carried out on Kieselgel-60 F 254 (Merck) 20×20 cm aluminium sheets for monitoring the compounds. 1D and 2D NMR data were recorded on a Varian Gemini 400 spectrometer at 400 MHz and 100 MHz for ^{1}H and ^{13}C nuclei, respectively at room temperature. All compounds were dissolved in deuterated chloroform ($CDCl_3$). Chemical shifts for signals were reported in parts per million (ppm) on the delta scale (δ), referenced to tetramethyl silane as the internal standard. The chemical shifts were referenced at δ_H 7.26 ppm in ^{1}H and δ_C 77.04 ppm in ^{13}C NMR for $CDCl_3$. Spin-spin coupling constants (*J*) were calculated in Hertz (Hz) and the splitting patterns were recorded as follows: *s*=singlet; *d*=doublet; *t*=triplet; *q*=quartet; *dd*=doublet of doublets; *m*=multiplet and *b*=broad.

Melting points (MP) were determined using a digital melting point apparatus (Stuart® SMP 20, Cole-Parmer, Staffordshire, UK), operated at 50 Hz and 75 W power and optical rotation was recorded on a Jasco P-2000 Polarimeter (JASCO, Germany). Infrared spectroscopy (IR) was carried out on a Fourier transform Spectrophotometer (PerkinElmer UATR Two, USA), in the range 400 cm^{-1} to 4000 cm^{-1} with a resolution of 4 cm^{-1} and 32 scans. The high-resolution electron spray ionization mass spectroscopic (HR-ESI-MS) data were acquired on a Bruker Daltonics Compact QTOF mass spectrometer in positive mode (ESI^{+}) using an electrospray ionization probe. The mass spectrometer was coupled to a thermal scientific ultimate 3000 Dionex UHPLC system consisting of an RS Auto Sampler WPS-3000, Pump HPG-3400 RS and detector DAD-3000 RS, using an Acclaim RSLC 120 C18, 2.2 μm, 2.1×100 mm (P/N 068982) column at 40 °C, flow rate 0.2 ml/min, solvent: Water-Acetonitrile (10:90, v/v) each solvent containing 0.1% of formic acid, isocratic condition, 5 min run. Processed spectra of all reported compounds are shown in supplementary materials 1.

Plant material

The plant *Rhoicissus tridentata* subsp. *cuneifolia* was purchased from a wildflower nursery in Hartbeespoort, S 05°04.579′ E 044°35.033′, North West province of South Africa. The plant specimen was identified by Erich Van Wyk and a voucher specimen was deposited at the South African National Biodiversity Institute (SANBI) in Pretoria (number 22,033).

Extraction and isolation

Dried and grounded roots plant material (1864.36 g) of *R. tridentata* was extracted sequentially with *n*-hexane, dichloromethane (DCM), ethyl acetate (EtOAc) and methanol (MeOH) for 48 h at temperatures between 15 and 25 °C, using a shaker. The extracts were filtered and concentrated under reduced pressure at 35 °C on a rotary evaporator to obtain a yield (2.59 g *n*-hexane, 3.61 g DCM, 4.55 g EtOAc and 71.28 g MeOH). Based on TLC analysis, the DCM crude extract was then subjected to repeated column chromatography (CC) using silica gel mixed with *n*-hexane and eluted with solvent systems, *n*-hexane: DCM (9:1, 8:2, 7:3 and 5:5 v/v). A total of 200 fractions were collected into 100 ml beakers and concentrated to dryness under a fume hood. Fraction F13D from the DCM crude extract showed interesting compounds with R_f values of 0.110 and 0. 231 as major compounds. This fraction afforded colorless crystals of sitosterol and 73.4 mg white powder of stigmasterol (**1**).

In vitrocytotoxicity assay

The resazurin assay

The cell viability after treatment with the Stigmasterol derivatives was assessed using the resazurin assay [37]. The triple negative breast cancer cell line (TNBC), HCC70 cells [oestrogen receptor (ER)-, progesterone receptor (PR)-, human epidermal growth factor-2 (HER-2)-] (ATCC: CRL-2315), was maintained in culture in RPMI-1640 media supplemented with 10% (v/v) heat-inactivated foetal bovine serum (FBS), 100 mg/ml streptomycin, 100 U/ml penicillin, 12.5 mg/ml amphotericin (PSA), 2 mM GlutaMAXTM and 2,5% (v/v) sodium bicarbonate. The hormone receptor-positive (ER^+, PR^+, $HER\text{-}2^-$), MCF-7 breast cancer cell line (ATCC: HTB-22) was maintained in Dulbecco's Modified Eagle's Medium (DMEM) supplemented with 10% (v/v) FBS, 100 U/ml PSA and 2 mM GlutaMAX™. The non-tumorigenic breast epithelial cell line MCF-12 A (ATCC: CRL-10,782) was maintained in DMEM:Hams F12 (1:1 ratio) supplemented in 10% (v/v) FBS, 500 ng/ml hydrocortisone, 100 U/ml PSA, 100 ng/ml cholera toxin, 10 mg/ml insulin and 20 ng/ml human epidermal growth factor (hEGF). All cells were maintained at 37 °C in a humidified 9% CO_2 incubator. The HCC70, MCF-7 and MCF-12 A cells were seeded at 5000 cells/well in a 96 well plate and were left overnight in a 9% CO_2 incubator at 37 °C to adhere. The cells were then treated with the synthetic compounds at a concentration range from 0.16 to 500.00 µM or with a vehicle control [0.2% (v/v) DMSO] for 96 h at 37˚C in a 9% CO_2 incubator. Thereafter, into each well, a solution of 10 µL of a 0.54 mM resazurin was added, followed by incubation for 2–4 h. Solubilization solution (10% (w/v) SDS in 0.01 M HCl) was then added overnight. 0.54 nM of resazurin solution was added and the cells were incubated for 2–4 h at 37˚C in a 9% CO2 incubator. The fluorescence was then measured on a Spectramax spectrophotometer with excitation and emission wavelength set at 560 and 590 nm respectively. The experiment was repeated in technical triplicate and the data was analysed using GraphPad Prism Inc, (USA) with half-maximal effective concentration (EC_{50} values) determined by non-linear regression. Selectivity index values for the compounds were calculated as follows: (EC_{50} of compound against MCF12A cells) ÷ (EC_{50} of compound against breast cancer cells) where a SI > 1 is indicative of selective toxicity towards cancer cells vs. non-cancerous cells.

Methods for the synthesis of stigmasterol derivatives

Acetylation procedure of stigmasterol

Pyridine (0.14 mL) and acetic anhydride (6 mL) were added to compound **1** (Stigmasterol) (0.739 g, 1.7907 mmol) in a 50 mL round-bottomed flask. The mixture was left to stir for 24 h at room temperature. The reaction was quenched with deionized water (10 mL) and was extracted with DCM (3×10 mL). The organic phase was washed with 2 M HCl (3×10 mL) to wash away excess pyridine and dried over anhydrous magnesium sulphate, filtered, and concentrated in *vacuo*. The residue was purified by column chromatography using *n*-Hexane: ethyl acetate (EtOAc) (98:2%) to afford compound **2** [38, 39].

Oxidation procedure of stigmasterol

To a solution of compound **1** (1.002 g, 2.4280 mmol) in acetone (24.28 mL) at 0 °C, Jones reagent (CrO_3/H_2SO_4) (1.94 mL) was added drop-wise. The reaction mixture was stirred at temperatures between 15 and 25 °C for 22 h. Isopropyl alcohol was added dropwise to remove excess Jones reagent, indicated by the appearance of a deep green colour. Upon completion, 5 mL of water was added before extraction with diethyl ether (2×30 mL). The combined ether layers were washed twice with sodium bicarbonate and brine, dried over anhydrous magnesium sulphate, and concentrated *in vacuo* [40]. The residue was purified by column chromatography using *n*-Hex: EtOAc (80:20%) to give compound **3** [39].

Epoxidation of stigmasterol

To a stirred solution of compound **1** (2.003 g, 4.8535 mmol) in DCM (49 mL) at temperatures between 15 and 25 °C was added *meta*-chloroperbenzoic acid (*m*CPBA) (4.1879 g, 24.2676 mmol). The reaction mixture was stirred for 24 h under N_2 inert conditions. 5 mL of water was then added to the reaction mixture and extracted with DCM (2×30 mL) [39]. The organic phase was washed successively with 10% aqueous sodium metabisulphite (3×10 mL) and saturated sodium bicarbonate (3×20 mL), dried over anhydrous sodium sulphate, and concentrated *in vacuo*. The crude product was purified by column chromatography using *n*-Hex: EtOAc (95:5%) to give compound **4**.

Dihydroxylation of compound 4 (5,6-epoxystigmast-22-en-3β-ol)

To a mixture of *N*-methylmorpholine-*N*-oxide.$2H_2O$ (0.56 g, 4.7540 mmol), deionized water (2.9 mL), acetone (1.1 mL) and osmium tetroxide (21 µL) was added to the epoxide **4** (1.019 g, 2.3770 mmol). The reaction was initially slightly exothermic and was maintained at temperatures between 15 and 25 °C with a water bath. After stirring overnight at room temperature under nitrogen, the reaction was complete. 5 mL of sodium sulphite was used to quench the reaction. The reaction mixture was then extracted with EtOAc (2×30 mL). The organic phase was washed successively with saturated sodium bicarbonate (3×20 mL) and brine (30 mL), dried over anhydrous sodium sulphate, and concentrated *in vacuo*.

The crude product was purified by column chromatography using *n*-Hex: EtOAc (80:20%) to give compound **5** [41].

Epoxide (4) ring-opening

To a suspension of the epoxide (compound **4**) (0.5860 g, 1.3670 mmol) in THF (9.1 mL) and H_2O (5.5 mL) at temperatures between 15 and 25 °C, $HClO_4$ (70% in H_2O, 120 µL) was added. After 50 min, $NaHCO_3$ (20 mL, saturated) was added, and the aqueous layer was extracted with ether (4×20 mL). The combined organic extracts were washed with saturated sodium bicarbonate (30 mL) and brine (30 mL), dried over anhydrous sodium sulphate and evaporated to give a white oil. The crude product was purified by column chromatography using *n*-Hex: EtOAc (80:20%) to give compound **6** [42].

Oxidation of compound 6 (stigmastane-3β,5,6,22,23-pentol)

To a solution of compound **6** (0.453 g, 0.9430 mmol) in acetone (9.4 mL) at 0 °C was added Jones reagent (CrO_3/H_2SO_4) (0.38 mL) in a drop-wise manner. The reaction mixture was stirred at temperatures between 15 and 25 °C for 22 h. Isopropyl alcohol was added dropwise to remove excess Jones reagent, indicated by the appearance of a deep green colour. Upon completion, 5 mL of water was added before extraction with ether (2×30 mL). The combined ether layer was washed twice with sodium bicarbonate and brine, dried over anhydrous magnesium sulphate, and concentrated *in vacuo* [40]. The residue was purified by column chromatography using *n*-Hex: EtOAc (80:20%) to give compound **7**, compound **8** and compound **9**.

Spectral data

Stigmasterol (1)

White powder, mp; 165–168 °C, $[\alpha]_D^{25}$ +64.34 ($CHCl_3$, Conc=4.51 (w/v %), $[M+H]^+$*m/z* 413.2688 ($C_{29}H_{48}O$) calculated for *m/z* 412.3705. IR; 2929 cm^{-1}, 2858 cm^{-1} (C-H), 1464 cm^{-1} (C=C), 3426 cm^{-1} (OH). ^{1}H NMR ($CDCl_3$, 400 MHz), δ_H (*ppm*); 3.51 (*m*, H-3), 5.04 (*dd, J*=8.50 Hz, 15.0 Hz, H-23), 5.17 (*dd, J*=8.60 Hz, 15.8 Hz, H-22), 5.34 (*d, J*=5.40 Hz, H-6), 0.69 (*s*, 3 H-18), 0.83 (*d, J*=6.6 Hz, 3 H-27), 0.81 (*d, J*=7.3 Hz, 3 H-26), 1.07 (*dd, J*=13.4 Hz, 4.8 Hz, 3 H-21) and 0.80 (*t, J*=7.2 Hz, 3 H-29). ^{13}C-NMR ($CDCl_3$, 100.6 MHz), δc (*ppm*); 37.2 (C-1), 31.6 (C-2), 71.8 (C-3), 42.3 (C-4), 140.7 (C-5), 121.7 (C-6), 31.9 (C-7), 31.6 (C-8), 50.1 (C-9), 36.5 (C-10), 21.1 (C-11), 40.5 (C-12), 42.2 (C-13), 56.8 (C-14), 24.3 (C-15), 29.3 (C-16), 56.1 (C-17), 12.2 (C-18), 19.7 (C-19), 40.5 (C-20), 21.2 (C-21), 138.3 (C-22), 129.2 (C-23), 51.2 (C-24), 33.9 (C-25), 19.3 (C-26), 21.1 (C-27), 25.4 (C-28), 12.0 (C-29).

Stigmasterol acetate (2)

^{1}H NMR (400 MHz, $CDCl_3$, δ *ppm*): 4.52 (1H, m, 3-H), 5.31 (1H, d, *J*=5.1 Hz, 6-H), 5.06 (1H, dd, *J*=15.2, 8.6 Hz, 22-H), 4.98 (1H, dd, *J*=15.1, 8.5 Hz, 23-H), 1.96 (3H, s, 2'-H).

^{13}C NMR (100.6 MHz, $CDCl_3$, δ *ppm*): 37.01 (C-1), 28.92 (C-2), 74.00 (C-3), 42.22 (C-4), 139.66 (C-5), 122.65 (C-6), 31.90 (C-7), 31.87 (C-8), 50.06 (C-9), 36.61 (C-10), 21.23 (C-11), 38.13 (C-12), 40.51 (C-13), 56.79 (C-14), 21.45 (C-15), 25.42 (C-16), 55.94 (C-17), 12.06 (C-18), 19.32 (C-19), 39.64 (C-20), 21.10 (C-21), 138.33 (C-22), 129.29 (C-23), 51.25 (C-24), 27.78 (C-25), 21.02 (C-26), 19.00 (C-27), 24.37 (C-28), 12.26 (C-29), 170.56 (C-1'), 21.02 (C-2').

Stigmasta-5,22-dien-3,7-dione (3)

^{1}H NMR (400 MHz, $CDCl_3$, δ *ppm*): 6.16 (1 H, s, 6-H), 5.11 (1 H, dd, *J*=15.2, 8.5 Hz, 22-H), 5.04 (1 H, dd, *J*=15.2, 8.5 Hz, 23-H).

^{13}C NMR (100.6 MHz, $CDCl_3$, δ *ppm*): 39.01 (C-1), 34.17 (C-2), 199.44 (C-3), 46.76 (C-4), 161.03 (C-5), 125.43 (C-6), 202.26 (C-7), 46.76 (C-8), 50.98 (C-9), 39.80 (C-10), 24.01 (C-11), 35.52 (C-12), 42.39 (C-13), 55.74 (C-14), 25.36 (C-15), 28.66 (C-16), 56.64 (C-17), 12.06 (C-18), 17.49 (C-19), 40.35 (C-20), 21.15 (C-21), 137.77 (C-22), 129.75 (C-23), 51.22 (C-24), 31.83 (C-25), 20.85 (C-26), 18.96 (C-27), 24.01 (C-28), 12.22 (C-29).

5,6-Epoxystigmast-22-en-3β-ol (4)

^{1}H NMR (400 MHz, $CDCl_3$, δ *ppm*): 3.84 (1 H, tt, *J*=10.8, 4.8 Hz, 3-H), 2.83 (1 H, d, *J*=4.3 Hz, 6-H), 5.06 (1 H, dd, *J*=15.2, 8.5 Hz, 22-H), 4.93 (1 H, dd, *J*=15.2, 8.5 Hz, 23-H).

^{13}C NMR (100.6 MHz, $CDCl_3$, δ *ppm*): 34.88 (C-1), 29.90 (C-2), 68.73 (C-3), 42.61 (C-4), 65.72 (C-5), 59.30 (C-6), 32.42 (C-7), 31.10 (C-8), 51.22 (C-9), 39.32 (C-10), 21.10 (C-11), 39.89 (C-12), 42.24 (C-13), 56.97 (C-14), 24.13 (C-15), 28.82 (C-16), 55.64 (C-17), 12.06 (C-18), 18.99 (C-19), 40.47 (C-20), 20.65 (C-21), 138.23 (C-22), 129.34 (C-23), 51.22 (C-24), 31.88 (C-25), 21.18 (C-26), 15.94 (C-27), 28.76 (C-28), 12.25 (C-29) [39].

5,6-Epoxystigmasta-3β,22,23-triol (5)

^{1}H NMR (400 MHz, $CDCl_3$, δ *ppm*): 3.88 (1 H, tt, *J*=11.2, 4.8 Hz, 3-H), 2.89 (1 H, d, *J*=4.4 Hz, 6-H), 3.68 (1 H, dd, m, 22-H), 3.48 (1 H, m, 23-H).

^{13}C NMR (100.6 MHz, $CDCl_3$, δ *ppm*): 38.67 (C-1), 29.89 (C-2), 65.71 (C-3), 42.67 (C-4), 63.04 (C-5), 62.06 (C-6), 32.39 (C-7), 31.04 (C-8), 56.45 (C-9), 34.85 (C-10), 20.82 (C-11), 39.81 (C-12), 48.25 (C-13), 59.25 (C-14), 20.92 (C-15), 29.12 (C-16), 58.55 (C-17), 11.83(C-18), 19.35 (C-19), 39.19 (C-20), 15.89 (C-21), 69.33 (C-22), 68.61 (C-23), 55.76 (C-24), 29.12 (C-25), 15.89 (C-26), 16.24 (C-27), 20.92 (C-28), 12.34 (C-29).

Stigmastane-3β,5,6,22,23-pentol (6)

^{1}H NMR (400 MHz, $CDCl_3$, δ *ppm*): 4.09 (1 H, dd, *J*=11.5, 6.3 Hz, 3-H), 3.53 (1 H, s, 6-H), 2.73 (1 H, dd, *J*=7.2, 2.3 Hz, 22-H), 2.49 (1 H, m, 23-H).

^{13}C NMR (100.6 MHz, $CDCl_3$, δ *ppm*): 30.27 (C-1), 38.26 (C-2), 67.66 (C-3), 38.56 (C-4), 76.07 (C-5), 75.85 (C-6), 20.15 (C-7), 43.03 (C-8), 53.51 (C-9), 55.53 (C-10), 20.90 (C-11), 43.08 (C-12), 55.56 (C-13), 56.13 (C-14), 29.11 (C-15), 29.32 (C-16), 45.68 (C-17), 12.13 (C-18), 12.42 (C-19), 48.28 (C-20), 16.06 (C-21), 63.10 (C-22), 62.12 (C-23), 48.76 (C-24), 19.35 (C-25), 29.32 (C-26), 19.35 (C-27), 30.27 (C-28), 16.83 (C-29).

Stigmasta-5-en-3,7-dion-22,23-diol (7)

^{1}H NMR (400 MHz, $CDCl_3$, δ *ppm*): 6.16 (1 H, s, 6-H), 2.75 (1 H, d, *J*=2.4 Hz, 22-H), 2.74 (1 H, d, *J*=2.3 Hz, 23-H).

^{13}C NMR (100.6 MHz, $CDCl_3$, δ *ppm*): 38.92 (C-1), 39.75 (C-2), 199.35 (C-3), 46.70 (C-4), 160.84 (C-5), 125.52 (C-6), 202.06 (C-7), 42.81 (C-8), 46.70 (C-9), 35.51 (C-10), 20.92 (C-11), 34.16 (C-12), 39.75 (C-13), 53.26 (C-14), 29.15 (C-15), 29.33 (C-16), 50.90 (C-17), 11.88 (C-18), 12.40 (C-19), 34.16 (C-20), 16.02 (C-21), 61.87 (C-22), 56.16 (C-23), 48.27 (C-24), 19.61 (C-25), 29.33 (C-26), 20.13 (C-27), 29.67 (C-28), 16.02 (C-29).

Stigmasta-3,7-dion-5,6,22,23-ol (8)

^{1}H NMR (400 MHz, $CDCl_3$, δ *ppm*): 3.16 (1 H, *m*, 6-H), 2.89 (1 H, s, 22-H), 2.85 (1 H, s, 23-H).

^{13}C NMR (100.6 MHz, $CDCl_3$, δ *ppm*): 37.40 (C-1), 41.80 (C-2), 211.07 (C-3), 43.13 (C-4), 82.67 (C-5), 82.65 (C-6), 211.33 (C-7), 43.34 (C-8), 55.84 (C-9), 37.40 (C-10), 20.91 (C-11), 38.44 (C-12), 43.34 (C-13), 55.86 (C-14), 29.09 (C-15), 20.93 (C-16), 62.00 (C-17), 11.94 (C-18), 12.38 (C-19), 37.42 (C-20), 13.80 (C-21), 62.92 (C-22), 62.03 (C-23), 58.59 (C-24), 19.61 (C-25), 29.09 (C-26), 20.12 (C-27), 29.09 (C-28), 15.98 (C-29).

Stigmast-5-ene-3β,22,23-triol (9)

^{1}H NMR (400 MHz, $CDCl_3$, δ *ppm*): 4.33 (1 H, t, *J*=2.8 Hz, 3-H), 5.80 (1 H, s, 6-H), 2.75 (1 H, d, *J*=2.3 Hz, 22-H), 2.73 (1 H, d, *J*=2.3 Hz, 23-H).

^{13}C NMR (100.6 MHz, $CDCl_3$, δ *ppm*): 34.22 (C-1), 29.68 (C-2), 73.13 (C-3), 42.79 (C-4), 168.43 (C-5), 126.30 (C-6), 29.17 (C-7), 29.72 (C-8), 53.56 (C-9), 37.09 (C-10), 20.15 (C-11), 38.56 (C-12), 42.79 (C-13), 56.03 (C-14), 24.37 (C-15), 20.95 (C-16), 55.52 (C-17), 11.98 (C-18), 16.07 (C-19), 37.05 (C-20), 12.43 (C-21), 63.00 (C-22), 62.04 (C-23), 48.28 (C-24), 19.60 (C-25), 20.95 (C-26), 20.15 (C-27), 24.37 (C-28), 16.07 (C-29).

Results and discussion

Analogues of stigmasterol were synthesized with the aim of enhancing its anticancer activity through acetylation, epoxidation, epoxide ring opening, oxidation, and dihydroxylation reactions as shown in Scheme 1. The synthesis of the stigmasterol derivatives was possible because of the pharmacophores present in stigmasterol, such as alkene bonds in position C-5, C-6, and position C-22, C-23 in the alkyl substituent and the hydroxyl group in the position C-3.

Characterization of synthesized compounds

Eight stigmasterol derivatives were successfully synthesized namely; Stigmasterol acetate (**2**), Stigmasta-5,22-dien-3,7-dione (**3**), 5,6-Epoxystigmast-22-en-3*β*-ol (**4**), 5,6-Epoxystigmasta-3β,22,23-triol (**5**), Stigmastane-3*β*,5,6,22,23-pentol (**6**), Stigmasta-5-en-3,7-dion-22,23-diol (7), Stigmasta-3,7-dion-5,6,22,23-ol (**8**) and Stigmast-5-ene-3*β*,22,23-triol (**9**). The structures of the synthesized compounds are shown in Fig. 2.

Stigmasterol acetate (**2**) was obtained as a white solid (0.5323 g, 1.1715 mmol, 65%) with a melting point of 139–141 °C. The specific optical rotation was recorded as $[\alpha]_D^{18.0}$= -54.5° (c=2.73 (w/v%), $CHCl_3$). The Q-TOF mass spectrum showed a molecular ion $[M\text{-}Na]^-$ peak at *m/*z 431.3788 with the molecular formula of $C_{31}H_{50}O_2$. The IR spectrum showed a peak appearing at 2942.2 cm^{-1} attributed to C-H stretches, the (C=O) stretch was observed at 1729.2 cm^{-1}, the (C=C) stretch was observed at 1461.0 cm^{-1} and the absorption bands at 1026.2 cm^{-1} were due to a (C-O) stretching.

Compound **2** was confirmed by the shift of the oxymethine proton (H-3) from the upfield region at δ_H 3.45 ppm (tt, *J*=10.4, 4.3 Hz, 1 H) to a slightly downfield region at δ_H 4.52 ppm (m, 1 H) in the ^{1}H NMR spectrum assigned to H-3, confirming an acetate group. In the ^{13}C NMR spectrum a presence of downfield carbon resonance at δ_C 170.56 ppm was observed, typical of an acetate group. The NMR data of the derivative is comparable to the literature values reported by Foley et al. [39] for stigmasterol acetate (**2**).

Stigmasta-5,22-dien-3,7-dione (3) was obtained as a brown solid (0.4628 g, 1.1278 mmol, 46%) with a melting point of 152–155 °C. The specific optical rotation was recorded as $[\alpha]_D^{20.5}$= -86.7° (c=1.00, $CHCl_3$). The Q-TOF mass spectrum showed a molecular ion $[M+H]^+$ peak at *m/*z 425.3418 with the molecular formula of $C_{29}H_{44}O_2$. The absorption band at 2942.2 cm^{-1} in the IR spectrum was attributed to C-H stretches, the (C=O) stretch was observed at 1690.0 cm^{-1} and the (C=C) stretch was observed at 1461.0 cm^{-1}.

The ^{1}H NMR spectrum of the compound exhibited a sharp and long singlet at δ_H 6.16 ppm, attributed to the olefinic methine proton H-6. There was a chemical shift

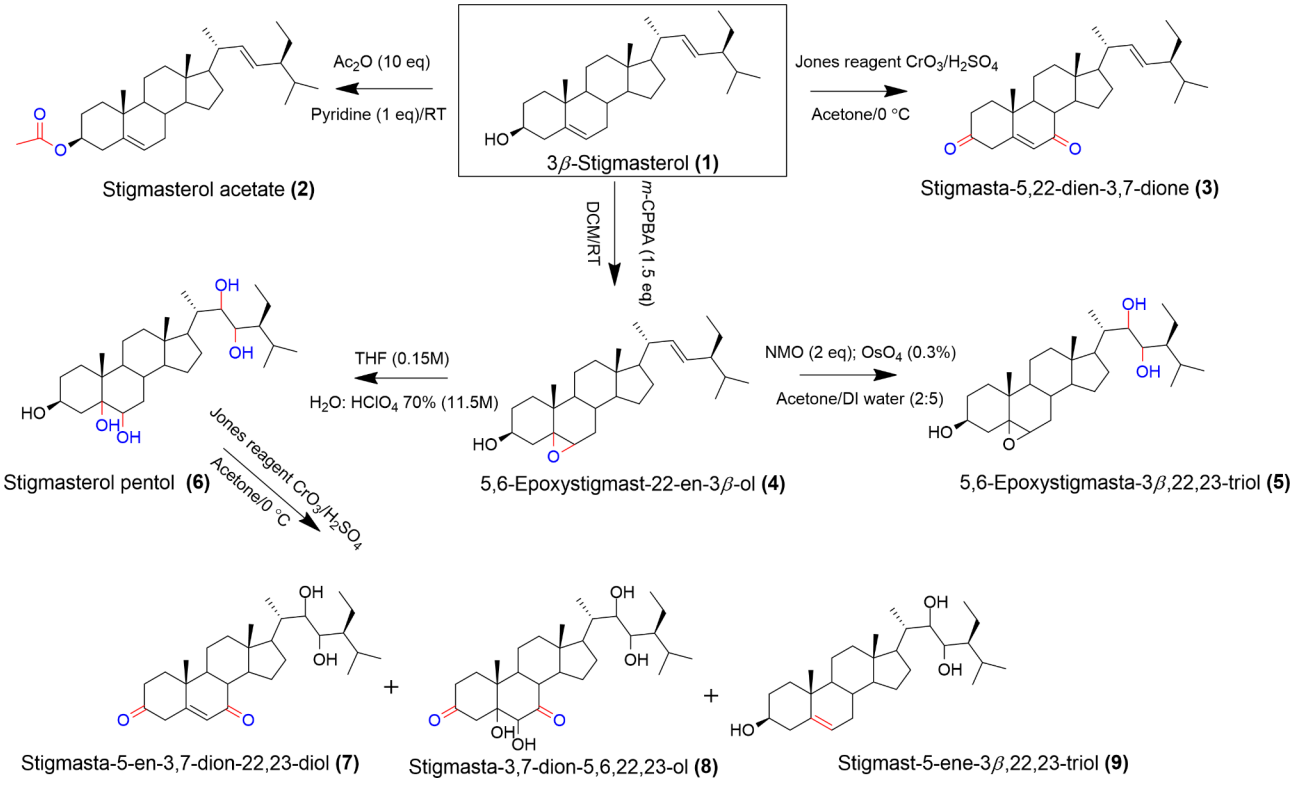

Scheme 1 Schematic representation of the synthesized stigmasterol derivatives

of the methine proton at position 6 from δ_H 5.28 ppm (d, *J*=4.9 Hz, 1 H) to δ_H 6.16 ppm. The absence of the oxymethine proton at δ_H 3.45 ppm (tt, *J*=10.4, 4.3 Hz, 1 H) of stigmasterol, in the ^{1}H NMR spectrum confirmed the formation of a carbonyl at position C-3 displaying a carbon resonance at δ_C 199.44 ppm. Moreover, the difference in the ^{13}C NMR spectra of the product and the starting material (stigmasterol) was the appearance of the signals at δ_C 199.44 and δ_C 202.26 ppm in the ^{13}C NMR spectrum of the product. The peaks were attributed to the keto carbonyl carbons at C-3 and C-7, respectively [39]. The proton at δ_H 2.48 ppm (H-4) was seen correlating to C-3 which confirmed the assignment of the carbonyl to C-3. These values are consistent with those reported by Donkwe et al. [35].

5,6-Epoxystigmast-22-en-3*β*-ol (4) was obtained as a clear oil (1.5641 g, 3.6513 mmol, 75%) with a melting point of 142–145 °C. The specific optical rotation was recorded as $[\alpha]_D^{20.7}$ = -60.2° (c=1.25, $CHCl_3$). The Q-TOF mass spectrum showed a molecular ion $[M+H]^+$ peak at *m/z* 429.3719 with the molecular formula of $C_{29}H_{48}O_2$. The IR spectrum showed a broad (-OH) peak appearing at 3452.3 cm^{-1}, the absorption band at 2935.7 cm^{-1} was attributed to C-H stretches and the (C=C) stretch was observed at 1729.2 cm^{-1}.

The disappearance of the olefinic proton at δ_H 5.28 ppm (d, *J*=4.9 Hz, 1 H) in H-6 of stigmasterol in the ^{1}H NMR spectrum and the appearance of the carbinol proton δ_H 2.83 ppm (d, *J*=4.3 Hz, 1 H) (H-6) in compound **4**, confirmed the successful epoxidation of stigmasterol. This was further confirmed by the disappearance of the alkene signals at 140.77 (C-5) and 121.73 (C-6) of the stigmasterol in the ^{13}C NMR spectrum. The resonances at C-5 and C-6 were shifted upfield to δ_C 65.72 ppm and δ_C 59.30 ppm, respectively in the ^{13}C NMR spectrum of compound **4** confirming the epoxy quaternary carbon resonances [39].

5,6-Epoxystigmasta-3*β*,22,23-triol (5) was obtained as a white solid (0.7230 g, 1.5637 mmol, 66%) with a melting point of 82–85 °C. The specific optical rotation was recorded as $[\alpha]_D^{20.3}$ = -51.7° (c=1.50, $CHCl_3$). The Q-TOF mass spectrum showed a molecular ion $[M+Na]^+$ peak at *m/z* 486.3954 with the molecular formula of $C_{29}H_{50}O_4$. The IR spectrum showed a broad (-OH) peak appearing at 3409.8 cm^{-1}, the absorption band at 2942.2 cm^{-1} was attributed to CH_2 stretching, the (C=O) stretch was observed at 1660.5 cm^{-1} and the absorption bands at 1062.1 cm^{-1} were due to a (C-O) stretching.

Compound **5** was confirmed by the appearance of oxymethine protons at δ_H 3.68 ppm and δ_H 3.48 ppm in the ^{1}H NMR spectrum of the product which was seen corresponding to C-22 and C-23. The absence of the olefinic protons at δ_H 5.06 ppm (dd, *J*=15.2, 8.5 Hz, 1 H) (H-22) and δ_H 4.93 ppm (dd, *J*=15.2, 8.5 Hz, 1 H) (H-23) of

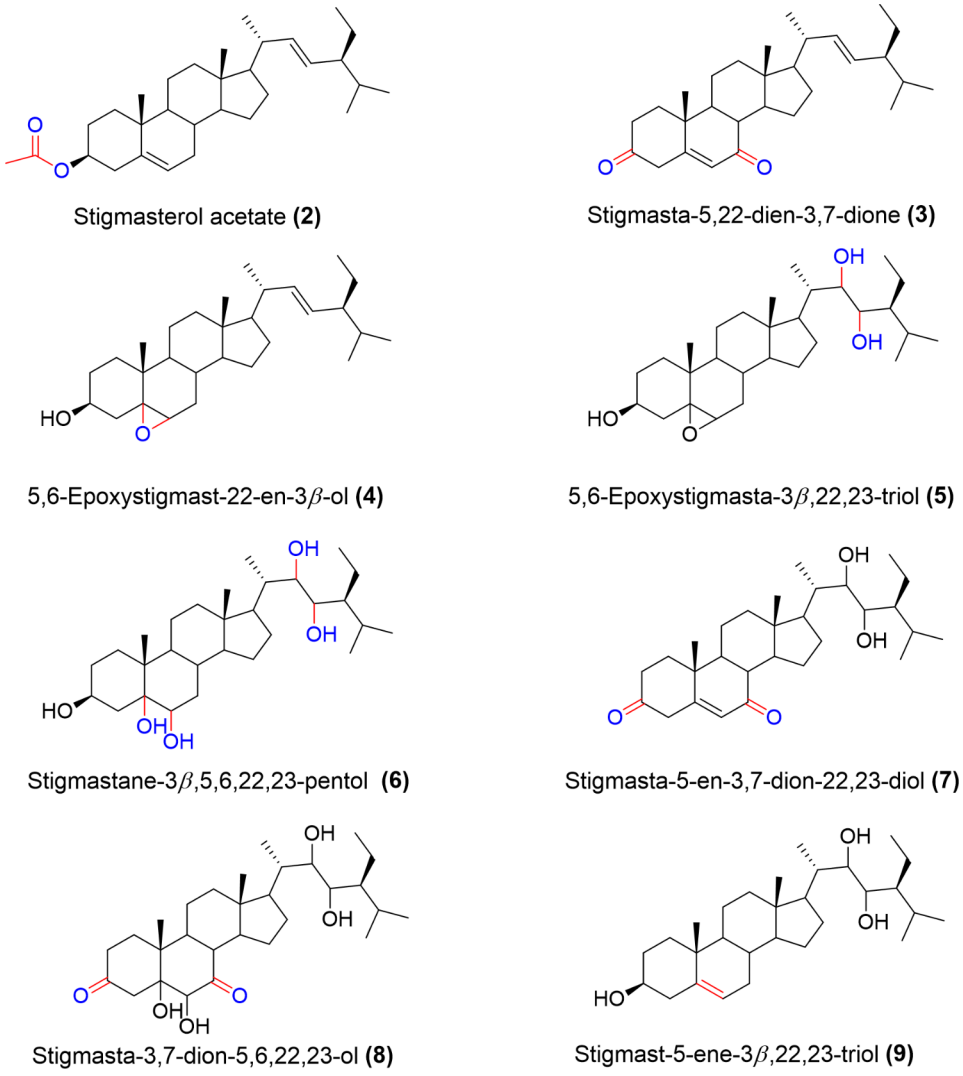

Fig. 2 Structures of synthesized stigmasterol derivatives

compound **4** in the ^{1}H NMR spectrum and the presence of the new oxymethine protons confirmed the successful addition of the hydroxyl groups at this position. This was further confirmed by the absence of olefinic carbon signals at δ_C 138.23 (C-22) and 129.34 (C-23), which were shifted upfield in the ^{13}C NMR spectrum of compound **5** [39].

Stigmastane-3*β*,5,6,22,23-pentol (6) was obtained as a colourless oil (0.533 g, 1.1095 mmol, 81%) with a melting point of 201–204 °C. The specific optical rotation was recorded as $[\alpha]_D^{20.1}$ = -29.6° (c=0.60, $CHCl_3$). The Q-TOF mass spectrum showed a molecular ion $[M\text{-}Na]^-$ peak at *m/z* 447.3738 with the molecular formula of $C_{29}H_{52}O_5$. The IR spectrum showed a broad (-OH) peak appearing at 3416.3 cm^{-1}, the absorption band at 2939.0 was attributed to C-H (alky) stretching and the absorption band at 1045.8 cm^{-1} was due to a (C-O) stretching.

The disappearance of the 2 olefinic protons at δ_H 5.06 ppm (dd, *J*=15.2, 8.5 Hz, 1 H) (H-22)and δ_H 4.93 ppm (dd, *J*=15.2, 8.5 Hz, 1 H) (H-23) of compound **4** and the appearance of 3 more oxymethine protons at δ_H 3.53 ppm, δ_H 2.73 ppm (dd, *J*=7.2, 2.3 Hz, 1 H) and δ_H 2.49 ppm confirmed the successful opening of the epoxide ring in compound **6**. The new oxymethine protons were seen corresponding to δ_C 75.85 ppm (C-6), δ_C 63.10 ppm (C-22) and δ_C 62.12 ppm (C-23) respectively in the HSQC spectrum. The proton at δ_H 3.53 ppm (H-6) was seen correlating to C-4 and the proton at δ_H 2.73 ppm (dd, *J*=7.2, 2.3 Hz, 1 H) (H-22) was seen correlating to C-20 and C-24 in the HMBC spectrum which confirmed the assignment of the hydroxyl groups at C-6, C-22 and C-23 [43].

Stigmasta-5-en-3,7-dion-22,23-diol (**7**) was obtained as a white powder (0.0947 g, 0.2131 mmol, 22%) with a melting point of 137–140 °C. The specific optical rotation

was recorded as $[\alpha]_D^{20.1}$ = -43.9° (c=0.85, $CHCl_3$). The Q-TOF mass spectrum showed a molecular ion $[M+H]^+$ peak at *m/*z 459.3487 with the molecular formula of $C_{29}H_{46}O_4$. The IR spectrum showed a broad (-OH) peak appearing at 3416.3 cm^{-1}, the absorption band at 2876.8 cm^{-1} was attributed to C-H stretching, the (C=C) stretch was observed at 1693.2 cm^{-1} and the absorption bands at 1735.7 cm^{-1} were due to a (C=O) stretching.

The structure of compound **7** was confirmed by the absence of the oxymethine proton at δ_H 4.09 ppm (dd, *J*=11.5, 6.3 Hz, 1 H) (H-3) of compound **6** and the appearance of a sharp and long singlet at δ_H 6.16 ppm attributed to an olefinic proton (H-6) in the ^{1}H NMR spectrum of compound **7**. Furthermore, there was an appearance of signals at δ_C 199.35 and δ_C 202.06 ppm in the ^{13}C NMR spectrum attributed to the keto carbonyl carbons C-3 and C-7, respectively. This is the first report of compound **7**.

Stigmasta-3,7-dion-5,6,22,23-ol (**8**) was obtained as a white solid (0.163 g, 0.3407 mmol, 36%) with a melting point of 183–187 °C. The specific optical rotation was recorded as $[\alpha]_D^{18.7}$= -26.9° (c=1.12, $CHCl_3$). The Q-TOF mass spectrum showed a molecular ion $[M+H]^+$ peak at *m/*z 495.3071 with the molecular formula of $C_{29}H_{48}O_6$. The IR spectrum showed a broad (-OH) peak appearing at 3364.0 cm^{-1}, the absorption band at 2873.6 cm^{-1} was attributed to C-H stretching and the (C=O) stretch was observed at 1709.5 cm^{-1}.

The ^{1}H NMR spectrum of compound **8** showed a shift in the proton resonance of H-6 from δ_H 3.53 ppm to δ_H 3.16 ppm confirming the addition of a hydroxyl group at C-6. The absence of the oxymethine proton resonance at δ_H 4.09 ppm (dd, *J*=11.5, 6.3 Hz, 1 H) (H-3) of compound **6**, confirmed the introduction of a carbonyl at position C-3 in compound **8**. Furthermore, there was an appearance of signals at δ_C 211.07 ppm and δ_C 211.33 ppm in the ^{13}C NMR spectrum of compound **8** attributed to the keto carbonyl carbons C-3 and C-7. This is the first report of compound **8**.

Stigmast-5-ene-3*β*,22,23-triol (**9**) was obtained as a white solid (0.102 g, 0.2285 mmol, 24%) with a melting point of 181–183 °C. The specific optical rotation was recorded as $[\alpha]_D^{19.5}$= -6.5° (c=1.81, $CHCl_3$). The Q-TOF mass spectrum showed a molecular ion $[M-H]^-$ peak at *m/*z 445.3581 with the molecular formula of $C_{29}H_{50}O_3$. The IR spectrum showed a broad (-OH) peak appearing at 3403.3, the absorption band at 2870.3 cm^{-1} was attributed to C-H stretching and the (C=C) stretch was observed at 1683.4 cm^{-1}.

The ^{1}H NMR spectrum of compound **9** indicated that the oxymethine proton at δ_H 3.53 ppm (H-6) of compound **6** changed to an olefinic proton δ_H 5.80 ppm (H-6). There was also an appearance of olefinic carbon resonances at δ_C 168.43 ppm (C-5) and δ_C 126.30 ppm (C-6) in the ^{13}C NMR spectrum [39].

Cytotoxic activities of stigmasterol derivatives

Stigmasterol and all synthesized stigmasterol derivatives were screened in vitro against breast cancer cells including, the triple-negative breast cancer (HCC70), hormone receptor-positive breast cancer (MCF-7) and non-tumorigenic epithelial cell lines established from breast tissue (MCF-12 A) cell lines. Camptothecin was used as the positive control. The cytotoxicity data for all the synthetic derivatives are summarized in Table 1.

The synthesized stigmasterol analogues showed improved cytotoxic activity compared to the stigmasterol (**1**), which was not toxic to the cancer cell lines (EC_{50} > 250 μM). Overall, the stigmasterol derivatives [stigmasterol acetate (**2**), stigmasta-5,22-dien-3,7-dione (**3**), 5,6-epoxystigmast-22-en-3*β*-ol (**4**), 5,6-epoxystigmasta-3*β*,22,23-triol (**5**), stigmastane-3*β*,5,6,22,23-pentol (**6**), stigmasta-5-en-3,7-dion-22,23-diol (**7**), stigmasta-3,7-dion-5,6,22,23-ol (**8**) and stigmast-5-ene-3*β*,22,23-triol (**9**)], demonstrated either modest toxicity [for example, stigmasta-5,22-dien-3,7-dione (**3**): 42.85±1.32 and 67.73±1.26 against MCF-7 and HCC70 breast cancer cell lines] or were found to be nontoxic [for example, stigmasterol acetate (**2**): EC_{50}>250 μM) against all three of the cell lines] as illustrated in Table 1. The exceptions were 5,6-epoxystigmast-22-en-3*β*-ol (**4**), stigmastane-3*β*,5,6,22,23-pentol (**6**) and stigmast-5-ene-3*β*,22,23-triol (**9**), which showed reasonable cytotoxic activity against MCF-7 and HCC70 cell lines. 5,6-epoxystigmast-22-en-3*β*-ol (**4**) and stigmast-5-ene-3*β*,22,23-triol (**9**), displayed EC_{50} values of 21.92 and 22.94 μM, respectively against hormone responsive MCF-7 breast cancer cells, while stigmastane-3*β*,5,6,22,23-pentol (**6**) exhibited an EC_{50} value of 16.82 μM against the triple negative breast cancer HCC70 cell line. In terms of selectivity of the compounds for the latter cancer cell lines over the non-cancerous control cell line, only 5,6-epoxystigmast-22-en-3*β*-ol (**4**) and stigmast-5-ene-3*β*,22,23-triol (**9**) display selectivity indices above 2, indicating that these compounds are more toxic to cancer cells (in particular MCF-7 cells) versus non-cancerous cells. The role of the epoxide ring and the hydroxyl group differed among the cell types. The presence of an epoxide ring seemed to enhance the activity in studies against the hormone responsive MCF-7 breast cancer cells. An increase in the number of hydroxyl groups appeared to increase the cytotoxic activity of the derivatives when the derivatives were screened against the triple negative breast cancer HCC70 cell line. This is the first report on breast cancer studies of these stigmasterol derivatives.

Table 1 In vitro cytotoxicity results of the synthesized stigmasterol derivatives against MCF-12 A, MCF-7 and HCC70 breast cells

Compound name	MCF-12 A		MCF-7		HCC70	
	EC_{50} and Standard deviation (μM)	R^2	EC_{50} and Standard deviation (μM)	R^2	EC_{50} and Standard deviation (μM)	R^2
stigmasterol (**1**)	NT		NT		NT	
stigmasterol acetate (**2**)	NT		NT		NT	
stigmasta-5,22-dien-3,7-dione (**3**)	30.18 ± 1.24	0.93	42.85 ± 1.32 **SI**: 0.70	0.88	67.73 ± 1.26 **SI**: 0.45	0.91
5,6-epoxystigmast-22-en-3*β*-ol (**4**)	46.97 ± 1.18	0.94	21.92 ± 1.32 **SI**: 2.14	0.82	165.70 ± 1.30 **SI**: 0.28	0.85
5,6-epoxystigmasta-3*β*,22,23-triol (**5**)	30.18 ± 1.28	0.90	43.99 ± 1.40 **SI**: 0.69	0.84	33.69 ± 1.33 **SI**: 0.90	0.88
stigmastane-3*β*,5,6,22,23-pentol (**6**)	22.56 ± 1.22	0.93	44.14 ± 1.40 **SI**: 0.51	0.84	16.82 ± 1.17 **SI**: 1.34	0.96
stigmasta-5-en-3,7-dion-22,23-diol (**7**)	31.60 ± 1.12	0.93	23.16 ± 1.08 **SI**:1.36	0.95	170.10 ± 1.18 **SI**:0.19	0.80
stigmasta-3,7-dion-5,6,22,23-ol (**8**)	NT		NT		53.23 ± 1.06	0.97
stigmast-5-ene-3*β*,22,23-triol (**9**)	51.79 ± 1.13	0.92	22.94 ± 1.09 **SI**:2.26	0.94	44.54 ± 1.13 **SI**:1.16	0.91
DCM crude (*R. tridentate)*	96.37 ± 1.19	0.87	˃250		13.82 ± 1.12 **SI**: 6.97	0.87
Camptothecin (**nM**)	104.20 ± 1.03	0.99	103.80 ± 9.92 **SI**:1.00	0.99	83.17 ± 1.08 **SI**:1.25	0.99

Key: NT = not toxic (EC_{50} > 250 μM); SI = selectivity index

Conclusion

Eight derivatives (**2**–**9**) of stigmasterol (**1**) were successfully synthesized via acetylation, oxidation, epoxidation, ring-opening and dihydroxylation of the epoxide. The structures of all the compounds were determined using spectroscopic techniques and melting points. Stigmasta-5-en-3,7-dion-22,23-diol (**7**) and Stigmasta-3,7-dion-5,6,22,23-ol (**8**) are reported for the first time. Stigmasterol and all the synthesized derivatives were screened against non-tumorigenic epithelial cell lines established from breast tissue (MCF-12 A), hormone receptor-positive breast cancer (MCF-7) and triple-negative breast cancer (HCC70) cell lines. The synthesized stigmasterol analogues demonstrated increased cytotoxic activity overall compared to the stigmasterol (**1**), which was not toxic to the cancer cell lines (EC_{50} ˃ 250 μM). In particular, 5,6-epoxystigmast-22-en-3*β*-ol (**4**) and stigmast-5-ene-3*β*,22,23-triol (**9**) showed improved cytotoxic activity and a degree of selectivity against MCF-7 breast cancer cells, with EC_{50} values of 21.92 and 22.94 μM, respectively, and selectivity indices of 2.14 and 2.26, respectively. On the other hand, stigmastane-3*β*,5,6,22,23-pentol (**6**) demonstrated increased cytotoxicity against the triple negative breast cancer HCC70 cell line, with an EC_{50} value of 16.82 μM, although this compound was not selective. Structural modification has proven to be a valid strategy to increase the anticancer activity of stigmasterol since all the synthesized derivatives displayed greatly improved activity. This represents a solid starting point in the development of novel anticancer drugs. Stigmasterol derivatives have potential as candidates for novel anticancer drugs hence further study of these compounds is needed.

Supplementary Information

The online version contains supplementary material available at https://doi.org/10.1186/s12906-023-04137-y.

Supplementary Material 1

Acknowledgements

The authors acknowledge the Tshwane University of Technology and Rhodes University for providing all the necessary instrumentation conducted in this study and the National Research Foundation Research for providing financial support. Prof R Krause from Rhodes University South Africa is greatly acknowledged for access to equipment and the analysis of compounds.

Authors' contributions

NPD: Data curation, Methodology, Writing- Original draft preparation, VJT: Supervision, Conceptualization, Methodology, Writing- Original draft preparation, Writing- Reviewing and Editing, GHR: Methodology, Writing- Reviewing and Editing, DK: Methodology, Writing- Reviewing and Editing, GRN: Data curation, Methodology, CD: Data curation, Methodology, JAD: Methodology, Writing- Reviewing and Editing, XSN: Writing- Reviewing and Editing, AEM: Supervision, Conceptualization, Methodology, Writing- Reviewing and Editing.

Funding

This work was financially supported by South Africa, through the National Research Foundation Research grant under grant numbers TTK190403426633 (JdIM), grant number 121119 (NPD), TTK180409318728, grant number 117898 (VJT), Tshwane University of Technology (VJT) and Rhodes University (JdIM), South Africa.

Data availability

All data generated or analysed during this study are included in this published article [and its supplementary information files].

Declarations

Ethics approval and consent to participate

All the methods used in this study were performed in accordance with relevant guidelines and regulation as approved by the research ethics committee. The permission to collect *Rhoicissus tridentata* was granted by the South African National Biodiversity Institute (SANBI).

Consent for publication

Not applicable.

Competing interests

The authors declare no competing interests.

Author details

[1]Department of Chemistry, Tshwane University of Technology, Private Bag X680, Pretoria 0001, South Africa
[2]Department of Biochemistry and Microbiology, Female Cancers Research at Rhodes University (FemCR2U), Makhanda/Grahamstown 6140, South Africa
[3]Department of Physical Sciences, University of Kabianga, Kericho 2030, Kenya
[4]Department of Pharmaceutical Sciences, Sefako Makgatho Health Sciences University, Pretoria 0204, South Africa

Received: 10 March 2023 / Accepted: 23 August 2023
Published online: 11 September 2023

References

1. Van Wyk BE, Gericke N. People's plants: A guide to useful plants of Southern Africa. Briza publications; 2000.
2. Opoku AR, Geheeb-Keller M, Lin J, Terblanche SE, Hutchings A, Chuturgoon A, Pillay D. Preliminary screening of some traditional Zulu medicinal plants for antineoplastic activities versus the HepG2 cell line. Phytother Res. 2000;14(7):534–7. https://doi.org/10.1002/1099-1573(200011)14:7%3C534::AID-PTR661%3E3.0.CO;2-A.
3. Naidoo V, Chikoto H, Bekker LC, Eloff JN. Antioxidant compounds in *Rhoicissus tridentata* extracts may explain their antibabesial activity: research in action. South Afr J Sci. 2006;102(5):198–200. https://hdl.handle.net/10520/EJC96550.
4. Rakuambo NC, Meyer JJM, Hussein A, Huyser C, Mdlalose S, Raidani T. *In vitro* effect of medicinal plants used to treat erectile dysfunction on smooth muscle relaxation and human sperm. J Ethnopharmacol. 2006;105(1–2):84–8. https://doi.org/10.1016/j.jep.2005.10.008.
5. McGaw LJ, Eloff JN. Ethnoveterinary use of southern african plants and scientific evaluation of their medicinal properties. J Ethnopharmacol. 2008;119(3):559–74. https://doi.org/10.1016/j.jep.2008.06.013.
6. Mukundi MJ, Mwaniki NE, Ngugi MP, Njagi JM, Agyirifo SD, Gathumbi KP, Muchugi NA. *In vivo* anti-diabetic effects of aqueous leaf extracts of *Rhoicissus tridentata* in alloxan induced diabetic mice. J Dev Drugs. 2015;4:1–5. https://doi.org/10.4172/2329-6631.1000131.
7. Mamba P, Adebayo SA, Tshikalange TE. Anti-microbial, anti-inflammatory and HIV-1 reverse transcriptase activity of selected south african plants used to treat sexually transmitted diseases. Int J Pharmacognosy Phytochemical Res. 2016;8:1870–6. https://doi.org/10.1016/j.sajb.2017.01.126.
8. Lin J, Opoku AR, Geheeb-Keller M, Hutchings AD, Terblanche SE, Jäger K, Van Staden A. Preliminary screening of some traditional zulu medicinal plants for anti-inflammatory and anti-microbial activities. J Ethnopharmacol. 1999;68(1):267–74. https://doi.org/10.1016/S0378-8741(99)00130-0.
9. Opoku A, Maseko N, Terblanche S. The *in vitro* antioxidative activity of some traditional Zulu medicinal plants. Phytother Res. 2002;16(S1):51–6. https://doi.org/10.1002/ptr.804.
10. Brookes KB, Smith AN. Cytotoxicity of pregnancy-related traditional medicines. South Afr Med J. 2003;93(5):359–61. PMID: 12830599.
11. Brookes KB, Katsoulis LC. Bioactive components of *Rhoicissus tridentate*: a pregnancy-related traditional medicine: research letter. South Afr J Sci. 2006;102(5):267–72. https://hdl.handle.net/10520/EJC96537.
12. Dube NP, Siwe-Noundou X, Krause RWM, Kemboi D, Tembu VJ, Manicum AL. Review of the traditional uses, Phytochemistry, and pharmacological activities of *Rhoicissus* Species (Vitaceae). Molecules. 2021;26(8):2306. https://doi.org/10.3390/molecules26082306.
13. Xiao Z, Morris-Natschke SL, Lee KH. Strategies for the optimization of natural leads to anticancer drugs or drug candidates. Med Res Rev. 2016;36(1):32–91. https://doi.org/10.1002/med.21377.
14. Hashem S, Ali TA, Akhtar S, Nisar S, Sageena G, Ali S, Al-Mannai S, Therachiyil L, Mir R, Elfaki I, Mir MM. Targeting cancer signaling pathways by natural products: exploring promising anti-cancer agents. Biomed Pharmacother. 2022;150:113054. https://doi.org/10.1016/j.biopha.2022.113054.
15. Kaur N, Chaudhary J, Jain A, Kishore L. Stigmasterol: a comprehensive review. Int J Pharm Sci Res. 2011;2(9):2259.
16. Bakrim S, Benkhaira N, Bourais I, Benali T, Lee L-H, El Omari N, Sheikh RA, Goh KW, Ming LC, Bouyahya A. Health benefits and pharmacological Properties of Stigmasterol. Antioxidants. 2022;11(10):1912. https://doi.org/10.3390/antiox11101912.
17. Cabral CE, Klein MRST. Phytosterols in the treatment of hypercholesterolemia and prevention of cardiovascular diseases. Arquivos brasileiros de cardiologia. 2017;109:475–82. https://doi.org/10.5935/abc.20170158.
18. Sundararaman P, Djerassi C. A convenient synthesis of progesterone from stigmasterol. The Journal of Organic Chemistry. 1977;42(22):3633-4. https://doi.org/10.1021/jo00442a044 PMID: 915584.
19. Kasahara Y, Kumaki K, Katagiri S, Yasukawa K, Yamanouchi S, Takido M, Akihisa T, Tamura T. *Carthami flos* extract and its component, stigmasterol, inhibit tumour promotion in mouse skin two-stage carcinogenesis. Phytother Res. 1994;8(6):327–31. https://doi.org/10.1002/ptr.2650080603.
20. Batta AK, Xu G, Honda A, Miyazaki T, Salen G. Stigmasterol reduces plasma cholesterol levels and inhibits hepatic synthesis and intestinal absorption in the rat. Metabolism. 2006;55(3):292–9. https://doi.org/10.1016/j.metabol.2005.08.024.
21. Panda S, Jafri M, Kar A, Meheta BK. Thyroid inhibitory, antiperoxidative and hypoglycemic effects of stigmasterol isolated from *Butea monosperma*. Fitoterapia. 2009;80(2):123–6. https://doi.org/10.1016/j.fitote.2008.12.002.
22. Gabay O, Sanchez C, Salvat C, Chevy F, Breton M, Nourissat G, Wolf C, Jacques C, Berenbaum F. Stigmasterol: a phytosterol with potential anti-osteoarthritic properties. Osteoarthr Cartil. 2010;18(1):106–16. https://doi.org/10.1016/j.joca.2009.08.019.
23. Ghosh T, Maity TK, Singh J. Evaluation of antitumor activity of stigmasterol, a constituent isolated from *Bacopa monnieri* Linn aerial parts against Ehrlich Ascites Carcinoma in mice. Orient Pharm Experimental Med. 2011;11(1):41–9. https://doi.org/10.1007/s13596-011-0001-y.
24. Li K, Yuan D, Yan R, Meng L, Zhang Y, Zhu K. Stigmasterol exhibits potent antitumor effects in human gastric cancer cells mediated via inhibition of cell migration, cell cycle arrest, mitochondrial mediated apoptosis and inhibition of JAK/STAT signalling pathway. Journal of the Balkan Union of Oncology. 2018;23(5):1420-5. https://doi.org/10.3892/ol.2018.9439 PMID: 30570868.
25. Kim Y-S, Li X-F, Kang K-H, Ryu B, Kim SK. Stigmasterol isolated from marine microalgae *Navicula incerta* induces apoptosis in human hepatoma HepG2 cells. BMB Rep. 2014;47(8):433. https://doi.org/10.5483/bmbrep.2014.47.8.153.
26. Newill H, Loske R, Wagner J, Johannes C, Lorenz RL, Lehmann L. Oxidation products of stigmasterol interfere with the action of the female sex hormone 17β-estradiol in cultured human breast and endometrium cell lines. Mol Nutr Food Res. 2007;51(7):888–98. https://doi.org/10.1002/mnfr.200700025.
27. Ayaz M, Sadiq A, Wadood A, Junaid M, Ullah F, Khan NZ. Cytotoxicity and molecular docking studies on phytosterols isolated from *Polygonum hydropiper* L. Steroids. 2019;141:30–5. https://doi.org/10.1016/j.steroids.2018.11.005.
28. Kangsamaksin T, Chaithongyot S, Wootthichairangsan C, Hanchaina R, Tangshewinsirikul C, Svasti J. Lupeol and stigmasterol suppress tumor angiogenesis and inhibit cholangiocarcinoma growth in mice via downregulation of tumor necrosis factor-α. PLoS ONE. 2017;12(12):e0189628. https://doi.org/10.1371/journal.pone.0189628.
29. Ali H, Dixit S, Ali D, Alqahtani SM, Alkahtani S, Alarifi S. Isolation and evaluation of anticancer efficacy of stigmasterol in a mouse model of DMBA-induced skin carcinoma. Drug Des Devel Ther. 2015;9:2793. https://doi.org/10.2147/dddt.s83514. PMID: 26060396 PMCID: PMC4454197.
30. Pandey P, Bajpai P, Siddiqui MH, Sayyed U, Tiwari R, Shekh R, Mishra K, Kapoor VK. Elucidation of the chemopreventive role of stigmasterol against Jab1 in Gall bladder carcinoma. Endocr Metabolic Immune Disorders-Drug Targets. 2019;19(6):826–37. https://doi.org/10.2174/1871530319666190206124120.
31. Scholtysek C, Krukiewicz AA, Sharma KP, Sharma PC, Goldmann WH. Characterizing components of the saw *Palmetto Berry* Extract (SPBE) on prostate cancer cell growth and traction. Biochem Biophys Res Commun. 2009;379(3):795–8. https://doi.org/10.1016/j.bbrc.2008.11.114.

32. Sianipar NF, Hadisaputri YE, Assidqi K, Salam S, Yusuf M, Destiarani W, Purnamaningsih R, So IG. Characterization and investigation of stigmasterol isolated from rodent tuber mutant plant (*Typhonium flagelliforme*), its molecular docking as anticancer on MF-7 cells. Preprints. 2021;2021070278. https://doi.org/10.20944/preprints202107.0278.v1.
33. Salam S, Harneti D, Maharani R, Safari A, Hidayat AT, Lesmana R, Nafiah MA, Supratman U, Prescott TA, Shiono Y. Cytotoxic triterpenoids from *Chisocheton pentandrus*. Phytochemistry. 2021;187:112759. https://doi.org/10.1016/j.phytochem.2021.112759.
34. Bae H, Song G, Lim W. Stigmasterol causes ovarian cancer cell apoptosis by inducing endoplasmic reticulum and mitochondrial dysfunction. Pharmaceutics. 2020;12(6):488. https://doi.org/10.3390/pharmaceutics12060488.
35. Donkwe SMM, Happi EN, Wansi JD, Lenta BN, Devkota KP, Neumann B, Stammler HG, Sewald N. Oxidative burst inhibitory and cytotoxic activity of constituents of the fruits of *Odyendyea gabonensis*. Planta Med. 2012;78(18):1949–56. https://doi.org/10.1055/s-0032-1327878.
36. O'Callaghan YC, Foley DA, O'Connell NM, McCarthy FO, Maguire AR, O'brien NM. Cytotoxic and apoptotic effects of the oxidized derivatives of stigmasterol in the U937 human monocytic cell line. J Agric Food Chem. 2010;58(19):10793–8. https://doi.org/10.1021/jf1023017.
37. de la Mare J-A, Lawson JC, Chiwakata MT, Beukes DR, Edkins AL, Blatch GL. Quinones and halogenated monoterpenes of algal origin show antiproliferative effects against breast cancer cells *in vitro*. Investig New Drugs. 2012;30(6):2187–200. https://doi.org/10.1007/s10637-011-9788-0.
38. McCarthy FO, Chopra J, Ford A, Hogan SA, Kerry JP, O'Brien NM, Ryan E, Maguire AR. Synthesis, isolation and characterisation of β-sitosterol and β-sitosterol oxide derivatives. Org Biomol Chem. 2005;3(16):3059–65. https://doi.org/10.1039/b505069c.
39. Foley DA, O'Callaghan Y, O'Brien NM, McCarthy FO, Maguire AR. Synthesis and characterization of stigmasterol oxidation products. J Agric Food Chem. 2010;58(2):1165–73. https://doi.org/10.1021/jf9024745.
40. Harding KE, May LM, Dick KF. Selective oxidation of allylic alcohols with chromic acid. J Org Chem. 1975;40(11):1664–5. https://doi.org/10.1021/jo00899a040.
41. VanRheenen V, Kelly R, Cha DY. An improved catalytic OsO_4 oxidation of olefins to *cis*-1, 2-glycols using tertiary amine oxides as the oxidant. Tetrahedron Lett. 1976;17(23):1973–6. https://doi.org/10.1016/S0040-4039(00)78093-2.
42. Jin Q, Williams DC, Hezari M, Croteau R, Coates RM. Stereochemistry of the macrocyclization and elimination steps in taxadiene biosynthesis through deuterium labeling. J Org Chem. 2005;70(12):4667–75. https://doi.org/10.1021/jo0502091.
43. Misharin AY, Mehtiev AR, Morozevich GE, Tkachev YV, Timofeev VP. Synthesis and cytotoxicity evaluation of 22,23-oxygenated stigmastane derivatives. Bioorg Med Chem. 2008;16(3):1460–73. https://doi.org/10.1016/j.bmc.2007.10.056.

Publisher's Note